

Upper-bound for the Pairwise Error Probability of Space-time Codes in Physical Channel Scenarios

Tharaka A. Lamahewa, Rodney A. Kennedy and Thushara D. Abhayapala

Abstract—In this paper, we derive an upper-bound for the pair-wise error probability of space-time codes which captures the effects of the transmitter and the receiver antenna configurations (antenna separation and antenna geometry) and the surrounding scattering distributions at the transmitter and the receiver antenna arrays. This new upper-bound allows investigation of the individual effects of antenna configuration and scattering environment parameters on the performance of space-time codes. Using this upper-bound, we quantify the degree of the effect of antenna configuration on the diversity advantage given by a space-time code. Simulation results show that as the number of antennas increase within a fixed aperture, the diversity advantage of a space-time code is upper-limited by the size of the antenna aperture.

Index Terms—Chernoff upper-bound, modal correlation, MIMO system, non-isotropic scattering, space-time trellis code.

I. INTRODUCTION

The Chernoff upper-bound on pairwise error probability (PEP) over uncorrelated MIMO channels was originally derived in [1], by *Tarokh et al.* Based upon this upper-bound, design rules for space-time trellis codes were proposed.

Several approaches have been found in literature, where the upper-bound for PEP is applied to correlated MIMO channels, [2], [3]. However, with these approaches, the upper-bound is constrained by one of the following: the correlation is restricted to one end of the channel; antenna configuration is restricted to uniform linear arrays; the scattering distribution around the antenna aperture is confined to a particular scattering distribution. In [4], [5], an upper-bound for the PEP is derived considering correlations at both ends of the channel. However the bound presented there does not allow investigation of the individual effects of antenna spacing, antenna placement and scattering environments on space-time codes.

This work was supported by the Australian Research Council Discovery Grant DP0343804.

The authors are with the Department of Telecommunications Engineering, Research School of Information Sciences and Engineering, the Australian National University, Canberra ACT 0200, Australia, email: {tharaka.lamahewa, rodney.kennedy, thushara.abhayapala}@anu.edu.au. R.A. Kennedy and T.D. Abhayapala are also with National ICT Australia, Locked Bag 8001, Canberra, ACT 2601, AUSTRALIA. National ICT Australia is funded through the Australian Government's *Backing Australia's Ability* initiative, in part through the Australian Research Council.

In this paper, we present a generalized upper-bound for PEP on correlated MIMO channels, where the bound can be applied to any kind of antenna geometry and wide variety of scattering distributions at the receiver and the transmitter antennas. We discuss how this upper-bound deviates from the global upper-bound derived by *Tarokh et al* with the introduction of space (antenna separation and antenna placement) and surrounding scattering distributions. We quantify the number of antennas that can be employed in a given antenna aperture, without diminishing the diversity advantage of a space-time code, and show it is limited by the size of the antenna aperture.

The following notations are used in this paper. $[\cdot]^T$, $[\cdot]^*$ and $[\cdot]^\dagger$ denote the transpose, complex conjugate and conjugate transpose operations, respectively. The symbols $\delta(\cdot)$ and \otimes denote the Dirac delta function and Matrix Kronecker product, respectively. The matrix \mathbf{I}_n is the $n \times n$ identity matrix.

II. SYSTEM MODEL

Consider a MIMO system consisting of n_T transmit antennas and n_R receive antennas. Data transmitted from n_T transmit antennas are encoded by a space-time code \mathbf{X} , where \mathbf{X} is $n_T \times L$, L is the code length. Assuming quasi-static fading, the signals received at n_R receiver antennas during L symbol periods can be expressed in matrix form as

$$\mathbf{Y} = \sqrt{E_s} \mathbf{H} \mathbf{X} + \mathbf{N},$$

where E_s is the transmitted power per symbol at each transmit antenna, \mathbf{H} is the $n_R \times n_T$ zero-mean complex valued channel gain matrix, \mathbf{N} is the noise represented by $n_R \times L$ complex matrix in which entries are zero-mean independent Gaussian distributed random variables with variance $N_0/2$ per dimension and \mathbf{Y} is $n_R \times L$.

By taking into account physical aspects of scattering, the channel matrix \mathbf{H} can be decomposed into deterministic and random parts as [6] [7]

$$\mathbf{H} = \mathbf{J}_R \mathbf{H}_S \mathbf{J}_T^\dagger, \quad (1)$$

where \mathbf{J}_R and \mathbf{J}_T are deterministic and \mathbf{H}_S is a random matrix with complex normal Gaussian distributed entries. According to the channel model proposed in [6], \mathbf{H}_S is an i.i.d channel matrix, which has zero-mean unit

variance complex Gaussian entries, while \mathbf{J}_R and \mathbf{J}_T are associated to the receiver and transmitter antenna correlation matrices, respectively. In [7], \mathbf{H}_s represents the random non-isotropic scattering environment, while \mathbf{J}_R and \mathbf{J}_T represent the effect of antenna geometries at the receiver and transmitter antenna arrays, respectively. In the next section, we present the Chernoff upper-bound applied to correlated MIMO channels where the channel matrix \mathbf{H} has the decomposition (1).

III. CHERNOFF UPPER BOUND ON CORRELATED MIMO CHANNELS

Assume that perfect channel state information (CSI) is available at the receiver and maximum likelihood (ML) detection is employed at the receiver. Assume that the codeword \mathbf{X} was transmitted, but the ML-decoder chooses another codeword $\hat{\mathbf{X}}$. Then the PEP, conditioned on the channel, is upper bounded by the *Chernoff bound* [1]

$$P(\mathbf{X} \rightarrow \hat{\mathbf{X}}|\mathbf{h}) \leq \exp\left(-\frac{E_s}{4N_0} d_h^2(\mathbf{X}, \hat{\mathbf{X}})\right), \quad (2)$$

where $d_h^2(\mathbf{X}, \hat{\mathbf{X}}) = \mathbf{h}[\mathbf{I}_{n_R} \otimes \mathbf{C}_\Delta]\mathbf{h}^\dagger$, $\mathbf{C}_\Delta = (\mathbf{X} - \hat{\mathbf{X}})(\mathbf{X} - \hat{\mathbf{X}})^\dagger$, $\mathbf{h} = (\text{vec}(\mathbf{H}^T))^T$ a row vector and \mathbf{H} has the decomposition given in (1). To compute the average PEP, we average (2) over the joint distribution of \mathbf{h} . Assume that \mathbf{h} is a proper complex¹ $n_T n_R$ -dimensional Gaussian random vector with mean $\mathbf{0}$ and covariance matrix $\mathbf{R}_M = E\{\mathbf{h}^\dagger \mathbf{h}\}$, then the pdf of \mathbf{h} is given by [8]

$$p(\mathbf{h}) = \frac{1}{\pi^{n_T n_R} \det[\mathbf{R}_M]} \exp\{-\mathbf{h} \mathbf{R}_M^{-1} \mathbf{h}^\dagger\},$$

provided that \mathbf{R}_M is non-singular. Then the average PEP is bounded as follows

$$P(\mathbf{X} \rightarrow \hat{\mathbf{X}}) \leq \frac{1}{\pi^{n_T n_R} \det[\mathbf{R}_M]} \int \exp\{-\mathbf{h} \mathbf{R}_M^{-1} \mathbf{h}^\dagger\} d\mathbf{h} \quad (3)$$

where $\mathbf{R}_M^{-1} = \left(\frac{E_s}{4N_0} \mathbf{I}_{n_R} \otimes \mathbf{C}_\Delta + \mathbf{R}_M^{-1}\right)$. Assume \mathbf{R}_M is non-singular (positive definite), therefore the inverse \mathbf{R}_M^{-1} is positive definite, since the inverse matrix of a positive definite matrix is also positive definite [9, page 142]. Also note that \mathbf{C}_Δ is Hermitian and it has positive eigenvalues (through code construction, e.g. [1]), therefore \mathbf{C}_Δ is positive definite, hence $\mathbf{I}_{n_R} \otimes \mathbf{C}_\Delta$ is also positive definite. Therefore \mathbf{R}_M^{-1} is positive definite and hence \mathbf{R}_M is non-singular. Using the normalization property of Gaussian pdf

$$\frac{1}{\pi^{n_T n_R} \det[\mathbf{R}]} \int \exp\{-\mathbf{h} \mathbf{R}^{-1} \mathbf{h}^\dagger\} d\mathbf{h} = 1,$$

we can simplify (3) to

$$P(\mathbf{X} \rightarrow \hat{\mathbf{X}}) \leq \frac{\det[\mathbf{R}]}{\det[\mathbf{R}_M]} = \frac{1}{\det[\mathbf{R}^{-1} \mathbf{R}_M]},$$

¹To be proper complex, the mean of both the real and imaginary parts of \mathbf{H}_S must be zero and also the cross-correlation between real and imaginary parts of \mathbf{H}_S must be zero.

or equivalently

$$P(\mathbf{X} \rightarrow \hat{\mathbf{X}}) \leq \frac{1}{\det\left[\mathbf{I}_{n_T n_R} + \frac{E_s}{4N_0} \mathbf{R}_M [\mathbf{I}_{n_R} \otimes \mathbf{C}_\Delta]\right]}. \quad (4)$$

Substituting (1) for \mathbf{H} in $\mathbf{h} = (\text{vec}(\mathbf{H}^T))^T$ with Kronecker product identity [9, page 180] $\text{vec}(\mathbf{A}\mathbf{X}\mathbf{B}) = (\mathbf{B}^T \otimes \mathbf{A}) \text{vec}(\mathbf{X})$, we may write

$$\mathbf{R}_M = E\{\mathbf{h}^\dagger \mathbf{h}\} = E\left\{(\mathbf{J}_R^* \otimes \mathbf{J}_T) \mathbf{h}_S^\dagger \mathbf{h}_S (\mathbf{J}_R^T \otimes \mathbf{J}_T^\dagger)\right\},$$

where $\mathbf{h}_S = (\text{vec}(\mathbf{H}_S^T))^T$ is a row vector. In the above equation, \mathbf{J}_R and \mathbf{J}_T are deterministic matrices and \mathbf{h}_S is random. Therefore we write

$$\mathbf{R}_M = (\mathbf{J}_R^* \otimes \mathbf{J}_T) \mathbf{R}_S (\mathbf{J}_R^T \otimes \mathbf{J}_T^\dagger), \quad (5)$$

where $\mathbf{R}_S = E\{\mathbf{h}_S^\dagger \mathbf{h}_S\}$. For the channel model in [6], since the elements of \mathbf{H}_S are independent and identically distributed, $\mathbf{R}_S = \mathbf{I}$. For the channel model in [7], \mathbf{R}_S represents the covariance matrix of the scattering environment, which can either be correlated or uncorrelated, unlike the \mathbf{R}_S in [6].

In this work, we are interested in investigating the impact of antenna separation, antenna geometry and the scattering environment on the Chernoff upper-bound. The channel model given in [6] is restricted to a uniform linear array antenna configuration and a finite number of scatterers around the transmitter and receiver antenna arrays. However, the channel model given in [7], is capable of capturing different antenna geometries as well as various non-isotropic power distributions. Therefore, from here onwards, we use the 2-D spatial channel model² given in [7] to investigate the Chernoff upper-bound.

A. Spatial Channel Model

In the channel model of [7], \mathbf{J}_T is the $n_T \times (2M_T + 1)$ transmitter antenna configuration matrix and \mathbf{J}_R is the $n_R \times (2M_R + 1)$ receiver antenna configuration matrix, where $(2M_T + 1)$ and $(2M_R + 1)$ are the number of effective communication modes³ available at the transmitter and the receiver regions, respectively. Note that, M_T and M_R are determined by the size of the antenna aperture [10], but not from the number of antennas encompassed in an antenna array, and is given by $M = \lceil \pi e r / \lambda \rceil$, where $\lceil \cdot \rceil$ is the ceiling operator, r is the minimum radius of the antenna aperture, $e \approx 2.7183$ and λ is the wavelength. Finally, \mathbf{H}_S is the $(2M_R + 1) \times (2M_T + 1)$ random

²The 2-dimensional case is a special case of 3-dimensional case where all the signals arrive from horizontal plane only.

³The set of modes form a basis of functions for representing a multipath wave field.

scattering matrix with (ℓ, m) -th element given by

$$\{\mathbf{H}_S\}_{\ell,m} = \int_0^\pi \int_0^\pi g(\phi, \varphi) e^{-i(\ell-M_R-1)\varphi} e^{i(m-M_T-1)\phi} d\varphi d\phi \quad d_g = \min\{\text{rank}(\mathbf{J}_T)\text{rank}(\mathbf{J}_R), n_R \text{rank}(\mathbf{C}_\Delta)\}. \quad (6)$$

for $\ell = 1, \dots, 2M_R + 1$, $m = 1, \dots, 2M_T + 1$. Note that $\{\mathbf{H}_S\}_{\ell,m}$ represents the complex gain of the scattering channel between the m -th mode of the transmitter region and the ℓ -th mode of the receiver region, where $g(\phi, \varphi)$ is the scattering gain function which gives the effective random complex gain for signals leaving the transmitter aperture with angle of departure ϕ and arriving at the receiver aperture with angle of arrival φ .

B. Remarks on New Upper-bound

Following remarks can be made regarding the upper-bound (4) and its association with the space-time trellis codes.

i). Antenna geometries, both at the transmitter and the receiver regions are incorporated into the upper-bound through matrices \mathbf{J}_T and \mathbf{J}_R in (5). Correlation effects due to the surrounding non-isotropic scattering distributions are also captured by the inclusion of correlation matrix \mathbf{R}_S in (5). Upper-bound (4) together with the channel model [7] allows us to investigate the individual effects of antenna separation, antenna placement and scattering environment parameters such as mean angle-of-arrival (AOA) and angular spread on the performance space-time codes. Note that upper-bounds found in [4], [5] do not allow one to analyze the individual effects of above mentioned deterministic and random factors on space-time codes.

ii). *Tarokh et. al.*, in [1], has used the PEP upper-bound for uncorrelated channels to derive the design rules for space-time trellis codes, under the hypothesis of high SNR. In these design rules, the overall diversity advantage of the system, d_g , is associated with the rank of the code word difference matrix times the number of receiver antennas, i.e., $d_g = n_R \text{rank}(\mathbf{C}_\Delta)$. However using the new upper-bound, it is possible to show that the quantitative degree to which the diversity advantage of a space-time code is reduced due to the size of the antenna aperture, antenna geometry and scattering environment parameters.

At high SNRs, the upper-bound (4) becomes

$$P(\mathbf{X} \rightarrow \hat{\mathbf{X}}) \leq \frac{1}{\det \left[\frac{E_s}{4N_0} \mathbf{R}_M [\mathbf{I}_{n_R} \otimes \mathbf{C}_\Delta] \right]}, \quad (7)$$

and the overall diversity advantage of the system is given by the rank of $\mathbf{R}_M [\mathbf{I}_{n_R} \otimes \mathbf{C}_\Delta]$. Assume that scattering environment is uncorrelated⁴, i.e., $\mathbf{R}_S =$

⁴A similar analysis can be carried out for correlated scattering environments as done in [4]

$\mathbf{I}_{(2M_T+1)(2M_R+1)}$, then

If $\text{rank}(\mathbf{J}_T)\text{rank}(\mathbf{J}_R) < n_R \text{rank}(\mathbf{C}_\Delta)$, then the diversity advantage provided by the space-time code is reduced by the effect of transmitter and receiver antenna configuration matrices. Note that \mathbf{J}_T is $n_T \times (2M_T + 1)$ and \mathbf{J}_R is $n_R \times (2M_R + 1)$, where M_T and M_R are determined by the size of the transmitter and receiver regions [10], but not by the number of antennas encompassed in the region. Therefore, it is possible to have a situation where the number of effective modes available in a region are less than the number of antennas used in that region. Thus, in such a scenario, rank of the antenna configuration matrix is less than the number of antennas which are being used for transmission or reception, which will result in reduction of diversity advantage from that system.

C. Kronecker Product Model as a Special Case

In some circumstances, \mathbf{R}_S can be expressed as Kronecker product between two matrices [11]

$$\mathbf{R}_S = E \left\{ \mathbf{h}_S^\dagger \mathbf{h}_S \right\} = \mathbf{F}_R \otimes \mathbf{F}_T, \quad (8)$$

where \mathbf{F}_R and \mathbf{F}_T can be considered as correlation matrices observed at the receiver and the transmitter arrays, respectively.

Substituting (8) into (5) gives

$$\mathbf{R}_M = (\mathbf{J}_R^* \otimes \mathbf{J}_T) (\mathbf{F}_R \otimes \mathbf{F}_T) (\mathbf{J}_R^T \otimes \mathbf{J}_T^\dagger), \quad (9a)$$

$$= (\mathbf{J}_R^* \mathbf{F}_R \mathbf{J}_R^T) \otimes (\mathbf{J}_T \mathbf{F}_T \mathbf{J}_T^\dagger), \quad (9b)$$

where (9b) follows from (9a) by matrix identity [9, page 180] $(\mathbf{A} \otimes \mathbf{C})(\mathbf{B} \otimes \mathbf{D}) = \mathbf{AB} \otimes \mathbf{CD}$, provided that the matrix products \mathbf{AB} and \mathbf{CD} exist. Substituting (9b) into (4) yields the upper-bound

$$P(\mathbf{X} \rightarrow \hat{\mathbf{X}}) \leq \frac{1}{\det \left[\mathbf{I}_Q + \frac{E_s}{4N_0} (\mathbf{J}_R^* \mathbf{F}_R \mathbf{J}_R^T) \otimes (\mathbf{J}_T \mathbf{F}_T \mathbf{J}_T^\dagger \mathbf{C}_\Delta) \right]} \quad (10)$$

where $Q = n_T n_R$.

In the next section, we provide the conditions pertaining to factorization (8) for the channel model given in [7] and also the precise definitions of \mathbf{F}_R and \mathbf{F}_T . The upper-bound (10) will be used later in Section IV-B to analyze the correlation effects of scattering environment.

D. Transmitter and Receiver Modal Correlation

Using (6), we define the modal correlation between complex scattering gains as

$$\gamma_{m,m'}^{\ell,\ell'} \triangleq E \left\{ \{\mathbf{H}_S\}_{\ell,m} \{\mathbf{H}_S\}_{\ell',m'}^* \right\}.$$

Assume that the scattering from one direction is independent of that from another direction for both the receiver and the transmitter apertures. Then the second

order statistics of the scattering gain function $g(\phi, \varphi)$ can be defined as

$$E \{g(\phi, \varphi)g^*(\phi', \varphi')\} \triangleq G(\phi, \varphi)\delta(\phi - \phi')\delta(\varphi - \varphi'),$$

where $G(\phi, \varphi) = E \{|g(\phi, \varphi)|^2\}$ with normalization $\int \int G(\phi, \varphi)d\phi d\varphi = 1$. With the above assumption, the modal correlation coefficient, $\gamma_{m,m'}^{\ell,\ell'}$ can be simplified to

$$\gamma_{m,m'}^{\ell,\ell'} = \int \int G(\phi, \varphi)e^{-i(\ell-\ell')\varphi}e^{i(m-m')\phi}d\phi d\varphi.$$

Then the correlation between ℓ -th and ℓ' -th modes at the receiver region due to the m -th mode at the transmitter region can be given as

$$\gamma_{\ell,\ell'}^{Rx} = \int \mathcal{P}_{Rx}(\varphi)e^{-i(\ell-\ell')\varphi}d\varphi, \quad (11)$$

where $\mathcal{P}_{Rx}(\varphi) = \int G(\phi, \varphi)d\phi$ is the normalized azimuth power distribution of the scatterers surrounding the receiver antenna region. Here we see that modal correlation at the receiver is independent of the mode selected from transmitter region. Similarly, we define the correlation between m -th and m' -th modes at the transmitter as

$$\gamma_{m,m'}^{Tx} = \int \mathcal{P}_{Tx}(\phi)e^{i(m-m')\phi}d\phi, \quad (12)$$

where $\mathcal{P}_{Tx}(\phi) = \int G(\phi, \varphi)d\varphi$ is the normalized azimuth power distribution at the transmitter region. As for the receiver modal correlation, we can observe that modal correlation at the transmitter is independent of the mode selected from receiver region. Note that, azimuth power distributions $\mathcal{P}_{Rx}(\varphi)$ and $\mathcal{P}_{Tx}(\phi)$ can be modeled using all common power distributions such as Uniform, Gaussian, Laplacian, Von-Mises, etc.

Denoting the p -th column of scattering matrix \mathbf{H}_S as $\mathbf{H}_{S,p}$, the $(2M_R + 1) \times (2M_R + 1)$ receiver modal correlation matrix can be defined as

$$\mathbf{F}_R \triangleq E \left\{ \mathbf{H}_{S,p} \mathbf{H}_{S,p}^\dagger \right\},$$

where (ℓ, ℓ') -th element of \mathbf{F}_R is given by (11) above.

Similarly, the transmitter modal correlation matrix can be written as

$$\mathbf{F}_T = E \left\{ \mathbf{H}_{S,q}^\dagger \mathbf{H}_{S,q} \right\},$$

where $\mathbf{H}_{S,q}$ is the q -th row of \mathbf{H}_S . (m, m') -th element of \mathbf{F}_T is given by (12) and \mathbf{F}_T is a $(2M_T + 1) \times (2M_T + 1)$ matrix. The correlation between two distinct modal pairs can be given as the product of corresponding modal correlation at the transmitter and the modal correlation at the receiver, i.e.,

$$\gamma_{m,m'}^{\ell,\ell'} = \gamma_{\ell,\ell'}^{Rx} \gamma_{m,m'}^{Tx}. \quad (13)$$

Facilitating (13), we may write the correlation matrix of the scattering channel \mathbf{H}_S as the Kronecker product between the receiver modal correlation matrix and the transmitter modal correlation matrix,

$$\mathbf{R}_S = E \left\{ \mathbf{h}_S^\dagger \mathbf{h}_S \right\} = \mathbf{F}_R \otimes \mathbf{F}_T. \quad (14)$$

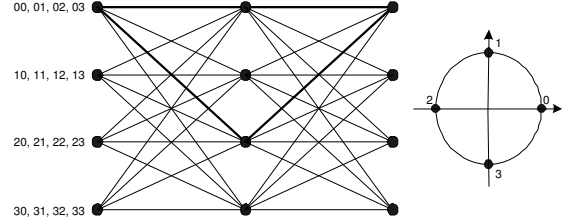
Note that (13) holds only for class of scattering environments where the power spectral density of modal correlation function satisfies [11], [12]

$$G(\phi, \varphi) = \mathcal{P}_{Tx}(\phi)\mathcal{P}_{Rx}(\varphi). \quad (15)$$

Note that, (15) is the necessary condition in which a channel must satisfy in order to hold the upper-bound (10), that we derived earlier in Section III-C.

IV. AN EXAMPLE

In this section, we compare the Chernoff bound derived in [1] with the new upper-bound, which caters for antenna spacing, antenna placement and surrounding scattering environments. As an example, we consider the QPSK 4-state space-time trellis code given in [1] for $n_T = 2$ antennas, which is illustrated in Fig.1. The labelling of the trellis branches follow [1]. The QPSK signal points are mapped to the edge label symbols as shown in Fig. 1.



1: Trellis diagram for 4-state space-time code for QPSK constellation.

Assume that the code word associated to all-zero sequence is transmitted, then the Chernoff upper-bound [1, Eq. (8)] for the shortest error event path of length $N = 2$, as illustrated by shading in Fig. 1, is found to be

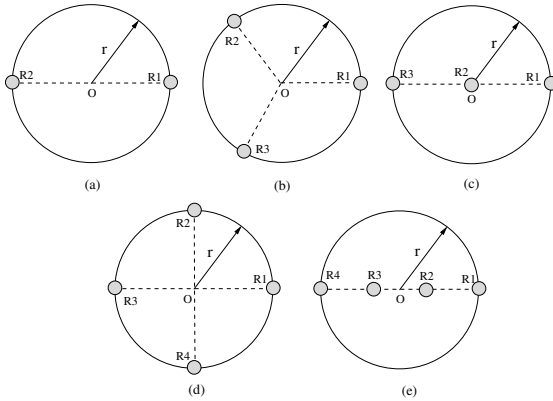
$$P(\mathbf{X} \rightarrow \hat{\mathbf{X}}) \leq \left(1 + \frac{E_s}{N_0} \right)^{-2n_R}. \quad (16)$$

A. Effects of antenna placement

First we consider the effect of space (antenna separation and placement) on the Chernoff upper-bound, when $\mathbf{R}_S = \mathbf{I}_{(2M_T+1)(2M_R+1)}$. Two transmitter antennas are placed half wavelength ($\lambda/2$) apart, which corresponds to $2\lceil \pi e 0.5 \rceil + 1 = 11$ effective communication modes at the transmitter aperture and $\text{rank}(\mathbf{J}_T) = 2$. Here we provide the simulation results of the upper-bound (4) for the shortest error event path of length 2 as shown in Fig. 1 for one, two, three and four receiver antennas. For each antenna system, the global upper-bound (16) is also plotted for comparison.

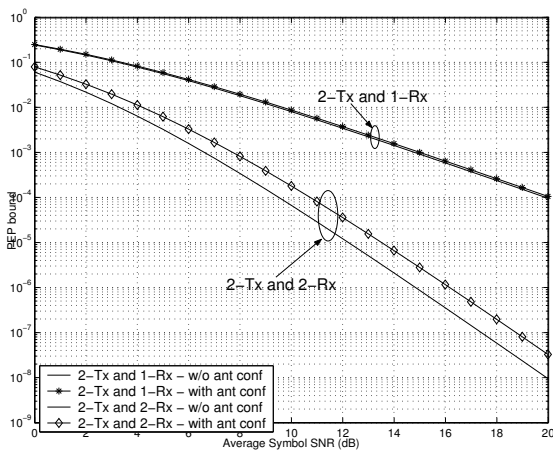
For the single receiver antenna case, we place the receiver antenna at the centre of the circular aperture. For the other three cases, receiver antennas are placed in a circular aperture with radius 0.1λ , as shown in Fig. 2. Note that $r = 0.1\lambda$ corresponds to $2\lceil \pi e 0.1 \rceil + 1 = 3$ effective communication modes at the receiver

aperture. With three and four receiver antenna cases, we also compare the behavior of the new upper-bound for different antenna geometries⁵ such as uniform circular array (UCA) and uniform linear array (ULA).



2: Receiver antenna configurations: (a) 2-Rx antennas are placed on x-axis, (b),(d) 3,4-Rx antennas are placed on an uniform circular array, (c), (e) 3,4-Rx antennas are placed on an uniform linear array.

Simulation results for 1 and 2 receiver antennas are shown in Fig. 3. With the single receiver antenna, the performance deviation between the new upper-bound and the global upper-bound is not significant. With two receiver antennas, the new upper-bound is 1-dB away from the global upper-bound. Fig. 3 shows that both the global upper-bound and the new upper-bound have the same slope, which indicates that two upper-bounds of the code have the same diversity advantage. However, for the 2×2 system a horizontal shift of the new upper-bound from global upper-bound is observed, which indicates a loss in coding gain due to the introduction of space.



3: Length 2 error event of 4-state QPSK space-time trellis code with two transmit antennas and n_R receive antennas ($n_R = 1, 2$).

Simulation results for 3 and 4 receiver antennas are

⁵The upper-bound developed here can be applied to any antenna configuration.

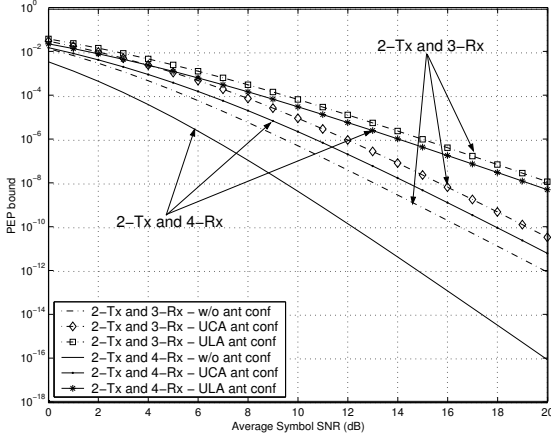
shown in Fig. 4. First we consider the three receiver antenna case. Three receiver antennas are placed in a UCA and are also placed in a ULA as depicted in Fig. 2(b) and Fig. 2(c), respectively. We found that $\text{rank}(\mathbf{J}_R) = 3$ for UCA and $\text{rank}(\mathbf{J}_R) = 2 (< n_R)$ for ULA. From Fig. 4 we observed that the performance deviation between the new upper-bound and the global upper-bound is significant for both UCA and ULA antenna configurations. For UCA antenna configuration we only observe a coding gain loss whereas for ULA antenna configuration we observe a coding gain loss as well as a diversity gain loss from the space-time code. Here the diversity loss from ULA is due to the loss of rank of \mathbf{J}_R , where $\text{rank}(\mathbf{J}_R)$ is less than the number of receiver antennas employed in the receiver array.

Now we consider the four receiver antenna case, where four receiver antennas are placed in a UCA and a ULA as depicted in Fig. 2(d) and Fig. 2(e), respectively. Fig. 4 shows that both antenna configurations reduce the diversity gain and the coding gain given by the code (c.f. with the global upper-bound). The expected diversity advantage from the 4-state QPSK space-time trellis code with 2-transmit and 4-receive antennas is 8. However, with the UCA antenna configuration, the overall diversity advantage given by the code is reduced to 6, as the rank of \mathbf{J}_R is 3 and with the ULA antenna configuration, it is reduced to 4 as the rank of \mathbf{J}_R is 2. This indicates that the diversity gain of a space-time coded system is governed by the rank of the antenna configuration matrix and the number of effective communication modes in the antenna aperture (directly related to the radius of the antenna aperture). In fact, the upper-limit for maximum number of antennas in an antenna aperture, without losing the diversity advantage of the space-time code, is given by the number of effective communication modes in that antenna aperture. However, if more than two antennas are aligned in a line, then further diversity reduction will be occurred (e.g. ULA case above).

Note that, performance deviations we see here are due to the introduction of space into the analysis of MIMO system and we have yet to consider the correlation effects of the scattering environment. In the next section we discuss the correlation effects of the scattering environment on the Chernoff upper-bound.

B. Effects of Scattering Environment Parameters

We now investigate the effect of modal correlation on the Chernoff upper-bound. For simplicity, we only consider the modal correlation at the receiver region and assume that the effective modes available at the transmitter are uncorrelated, i.e. $\mathbf{F}_{Tx} = \mathbf{I}_{2M_T+1}$. It was shown in [13] that, all azimuth power distributions (non-isotropic distributions) give very similar correlation values for a given angular spread. Therefore, without loss of generality, we restrict our investigation to Uniform limited azimuth power distribution (UL-APD) only. For the UL-APD, the modal correlation coefficient at the



4: Length 2 error event of 4-state QPSK space-time trellis code with two transmit antennas and n_R receive antennas ($n_R = 3, 4$).

receiver is given by

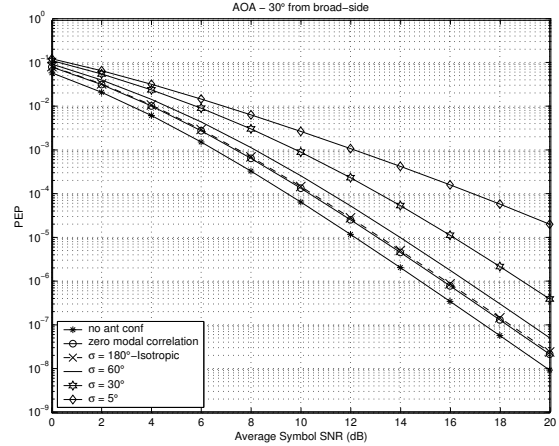
$$\gamma_{l,l'}^{Rx} = \text{sinc}((l-l')\Delta)e^{-i(l-l')\varphi_0},$$

where φ_0 is the mean angle of arrival (AOA) and Δ is the non-isotropic parameter of the power distribution, which is related to the angular spread σ . In this case, $\sigma = \Delta/\sqrt{3}$.

Consider a MIMO system consisting of two transmitter antennas and two receiver antennas. Antennas on each aperture are placed $(\lambda/2)$ apart and they are positioned on the x -axis relative to their aperture origin. Aperture radius $\lambda/2$ corresponds to 11 effective communication modes in each aperture and the rank of each antenna configuration matrix is 2. Therefore, this antenna configuration setup does not diminish the diversity advantage given by the code, however it reduces the coding gain due to the finite antenna spacing.

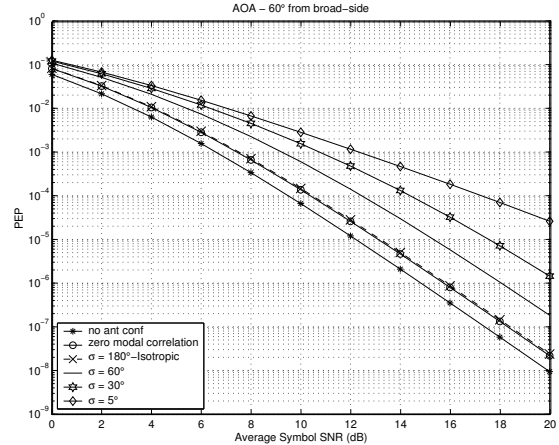
Simulation results of the new upper-bound are shown in Fig. 5, for mean AOA $\varphi_0 = 30^\circ$ from broadside. Angular spreads of $\sigma = [180^\circ, 60^\circ, 30^\circ, 5^\circ]$ have been considered. On the same figure, the global upper-bound and the new upper-bound without modal correlation effects are also super imposed. Note that, upper-bound for $\sigma = 180^\circ$, which represents the isotropic scattering, is overlapped with the bound with zero modal correlation, as expected.

As shown, the new upper-bound moves away from the global upper-bound as the angular spread σ decreases. At 10dB SNR, the new upper-bound is 2dB, 4dB and 8dB away from the global upper-bound for angular spreads $60^\circ, 30^\circ, 5^\circ$ respectively. The higher deviation of the new upper-bound from the global upper-bound at small angular spreads is due to the higher concentration of energy arriving closer to the mean AOA. This effect will make the MIMO channel to be rank deficient, hence the loss of diversity. Note that when $\sigma = 0^\circ$, the rank of the receiver modal correlation matrix will be 1, which results in no diversity advantage from the



5: Length 2 error event of 4-state QPSK space-time trellis code with two transmit antennas and two receive antennas for a Uniform limited power distribution with mean AOA 30° from broadside.

code. Fig. 6 shows the simulation results for mean AOA $\varphi_0 = 60^\circ$ from broadside and angular spreads of $\sigma = [180^\circ, 60^\circ, 30^\circ, 5^\circ]$. We observed that as the mean AOA moves away from the broadside, the new upper-bound moves further away from the global upper-bound.



6: Length 2 error event of 4-state QPSK space-time trellis code with two transmit antennas and two receive antennas for a Uniform limited power distribution with mean AOA 60° from broadside.

V. CONCLUSION

We derived an upper-bound for the pair-wise error probability of space-time codes which captures the effects of the transmitter and the receiver antenna configurations and the surrounding scattering distributions at the transmitter and the receiver antenna arrays. Using this upper-bound, we showed that the quantitative degree to which the diversity advantage of a space-time code is reduced by the size of the antenna aperture and the antenna configuration. We also showed that the diversity advantage and the coding advantage of a space-time code are decreased when the mean AOA of an impinging

signal moves away from the broadside, and also when the angular spread of the azimuth power distribution is small. We believe that, the new upper-bound derived in this paper can be used as a tool to develop a space-time pre-coder which is capable of compensating (fully or partially) for effects of antenna configuration and scattering environment.

REFERENCES

- [1] V. Tarokh, N. Seshadri, and A.R. Calderbank, "Space-time codes for high data rate wireless communication: performance criterion and code construction," *IEEE Trans. Info. Theory*, vol. 44, no. 1, pp. 744–765, Mar. 1998.
- [2] V.K. Nguyen and L.B. White, "Space-time coding in spatially correlated rayleigh fading channels," in *7th International Symposium on Digital Signal Processing and Communication Systems*, Coolangata, Australia, December 2003, pp. 44–48.
- [3] I. Bahceci, T.M. Duman, and Y. Altunbasak, "Space-time coding over correlated fading channels with antenna selection," submitted to *IEEE Transactions on Wireless Communications*, Nov. 2003.
- [4] H. Bölcskei and A.J. Paulraj, "Performance of space-time codes in the presence of spatial fading correlation," in *Asilomar Conf. on Signals, Systems, and Computers*, Pacific Grove (CA), Oct. 2000, vol. 1, pp. 687–693.
- [5] D. Gore, R. W. Heath Jr, and A.J. Paulraj, "Statistical antenna selection for spatial multiplexing systems," in *Proc. of IEEE International Conf. on Communications*, New York, USA, Apr. 28 - May 2 2002, vol. 1, pp. 450–454.
- [6] D. Gesbert, H. Bölcskei, D.A. Gore, and A.J. Paulraj, "Outdoor MIMO wireless channels: Models and performance prediction," *IEEE Trans. Communications*, vol. 50, no. 12, pp. 1926–1934, Dec. 2002.
- [7] T.D. Abhayapala, T.S. Pollock, and R.A. Kennedy, "Spatial decomposition of MIMO wireless channels," Paris, France, July 2003, vol. 1, pp. 309–312.
- [8] N.R. Goodman, "Statistical analysis based on a certain multivariate complex gaussian distribution (an introduction)," *Ann. Math. Statist.*, vol. 34, pp. 152–177, 1963.
- [9] G.H. Golub and C.F. Van Loan, *Matrix Computations*, The Johns Hopkins University Press, Baltimore and London, third edition, 1996.
- [10] H.M. Jones, R.A. Kennedy, and T.D. Abhayapala, "On dimensionality of multipath fields: Spatial extent and richness," in *Proc. IEEE Int. Conf. Acoust., Speech, Signal Processing, ICASSP'2002*, Orlando, Florida, May 2002, vol. 3, pp. 2837–2840.
- [11] J.P. Kermoal, L. Schumacher, K.I. Pedersen, P.E. Mogensen, and F. Frederiksen, "A stochastic mimo radio channel model with experimental validation," *IEEE Journal on Selected Areas in Communications*, vol. 20, no. 6, pp. 1211–1226, Aug. 2002.
- [12] T.S. Pollock, "Correlation Modelling in MIMO Systems: When can we Kronecker?," in *Proc. 5th Australian Communications Theory Workshop*, Newcastle, Australia, February 2004, pp. 149–153.
- [13] T.S. Pollock, T.D. Abhayapala, and R.A. Kennedy, "Introducing space into MIMO capacity calculations," *Journal on Telecommunications Systems*, vol. 24, no. 2, pp. 415–436, 2003.